# Choroid Characterization in EDI OCT Retinal Images Based on Texture Analysis

A. González-López, B. Remeseiro, M. Ortega and M. G. Penedo

*Departmento de Computación, Universidade da Coruña, A Coruña 15071, Spain*

Keywords: OCT, Retinal Images, Choroid, Texture Analysis, Pattern Recognition, Machine Learning.

Abstract: Optical Coherence Tomography (OCT) is a widely extended imaging technique in the opthalmic field for diagnostic purposes. Since layers composing retina can be identified in these images, several image processing-based methods have been presented to segment them automatically in these images, with the aim of developing medical-support applications. Recently, appearance of Enhanced Depth Imaging (EDI) OCT allows to tackle exploration of the choroid which provides high information of eye processes. Therefore, segmentation of choroid layer has become one of the more relevant problems tackled in this field, but it presents different features that rest of the layers. In this work, a novel texture-based study is proposed in order to show that textural information can be used to characterize this layer. A pattern recognition process is carried out by using different descriptors and a process of classification, considering marks performed by two experts for validation. Results show that characterization using texture features is effective with rates over 90% of success.

## 1 INTRODUCTION

Optical Coherence Tomography (OCT) is a standard imaging technique in the ophthalmologic field, which provides a cross sectional image of the retina in a non-invasive, real time fashion (Puzyeyeva et al., 2011). Experts use OCT retinal images to diagnose diseases, because retinal morphology can be identified effectively on them, explaining disease pathogenesis and progression. Nowadays, Enhanced Depth Imaging (EDI) OCT allows to better visualize the choroid, which is the vascular tissue located at the posterior part of the eye, between the retina and the sclera. Choroid provides oxygen and nourishment to the outer layers of the retina (Bill et al., 1983) and its changes have been hypothesized to be of critical importance in the pathophysiology of several retinal diseases, such as glaucoma (Yin et al., 1997), central serous chorioretinopathy (Imamura et al., 2009) or retinitis pigmentosa (Dhoot et al., 2013). Therefore, characterization and delimitation of this layer in the OCT retinal images is important to understand the natural processes of the eye, besides detecting potential eye diseases.

Although retinal segmentation is a widely studied problem, automatic choroidal layer detection has not been investigated in as much depth. A few methods for this task have been recently reported. In

(Kajić et al., 2013), a two stage elaborated statistical model is presented to automatically detect the choroidal boundaries in EDI OCT images. A two-stage active contour-based technique is used in (Lu et al., 2013) to segment the outer boundary of the choroid, but it requires the manual initialization of the contour, while another semiautomatic approach is also studied in (Hu et al., 2013). In (Alonso-Caneiro et al., 2013), a graph-based method obtains promising results, but a process of enhancement is considered, dependant of the instrument used for the image capture. Choroidal vessels were analyzed through a choroidal segmentation method in (Zhang et al., 2012), but the focus of this work was to quantify the vasculature rather than the choroidal thickness.

Since choroidal surface presents different visual properties than the rest of retinal layers, a texture-based characterization is interesting to be tackled, as a previous step for a future segmentation method for choroidal boundaries. Although texture information is included in previous work (Danesh et al., 2014), where a Gaussian Mixture Model of the image is built based on features extracted with the Discrete Wavelet Transform, and then used in the segmentation task, it has not been studied deeply which features are those that best describes this layer for a future and robust process of segmentation. With that purpose, this work presents a study of texture features that can be consi-

dered to characterize this layer, in order to determine those that must be used to represent information in this layer and design future process of segmentation and information extraction. As results show, choroid can be characterized effectively using textural information.

This paper is organized as follows: Section 2 explains the method designed for the characterization of the choroid. Section 3 describes materials and methods, while in Section 4 obtained results are presented. Finally, conclusions and future lines are presented in Section 5.

## 2 METHODOLOGY

As it was introduced in Section 1, this work aims to characterize choroidal layer using texture features, in order to allow a future segmentation process of this layer.

The process is described as follows: firstly, the image provided by the OCT scanner is preprocessed, in order to make it suitable for the method. Since choroid is located between the Retinal Pigment Epithelium-Bruch's Membrane complex (RPE-BM) and the sclera (see Figure 1), the region of interest (ROI) must be bounded. Thus, choroidal upper boundary is detected and only the area covering choroid and sclera is studied. After that, several windows are extracted from the image to build different texture descriptors. Since ophthalmologic experts have marked manually the boundary between the choroid and the sclera (marked in Figure 1 as Outer Choroid Boundary (OCB) ) over the images, extracted features can be used to perform a classification process, in order to characterize the choroidal layer. Thus, it is possible to perform a pattern recognition process to discriminate between regions belonging to the choroid and those located in the sclera. This process is reflected graphically in Figure 2.
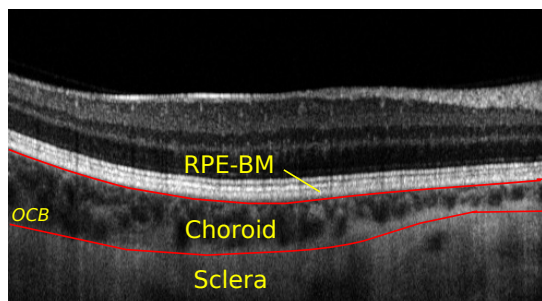


Figure 1: Sample OCT image with choroidal layer boundaries marked in red.

### 2.1 Preprocessing

Images provided by the OCT device includes irrelevant areas which must be excluded. Besides that, they are captured following an inverted gray-scale distribution than that used in the segmentation process needed in the ROI bounding step (Section 2.2). Thus, they are automatically cropped and inverted to make the following step feasible. It is essential to consider that image captured by the scanner is resized for a better visualization. This involves that, as it was observed during initial test, decreasing resolution of the images provided better results when texture features are extracted. Therefore, to tackle this process, after cropping images, they are resized using a scale factor of 0.5. Consequently, not only the effectiveness of the process is increased, but also the computation time is reduced.

### 2.2 ROI Location

As it was commented, ROI is determined by the area covering choroid and sclera. In order to bound it, the inner boundary of the choroid surface, corresponding to its borderline with the RPE-BC (see Figure 1), must be detected. With that purpose, the multistage active contour-based segmentation technique described in (González et al., 2014) is used. This method detects the boundary between these layers through a process of energy minimization.

In particular, the active contour model used to segment this boundary is described as follows:

- *Topology*: it is defined as a sequence of nodes covering the image width. Each node corresponds to one pixel in the image and has two neighbors, except for the first and the last ones. During the process of minimization, nodes can make displacements to its 8-connected neighbors (except for nodes in the extrema, which only can move along the rows in the image).

- *Internal energy*: first and second order terms are considered in order to guarantee continuity and curvature.

- *External energy*: since the boundary of interest can be identified as a light-to-dark transition in the image, besides the fact that it bounds a wide bright area (RPE-BC), it includes information of edges and regional intensity, as text belows explains.

The gradient distance is used, being computed over edges corresponding to the mentioned kind of transition. In order to avoid the influence of some edges that would make the model reaching wrong solutions and also for a fast evolution of the
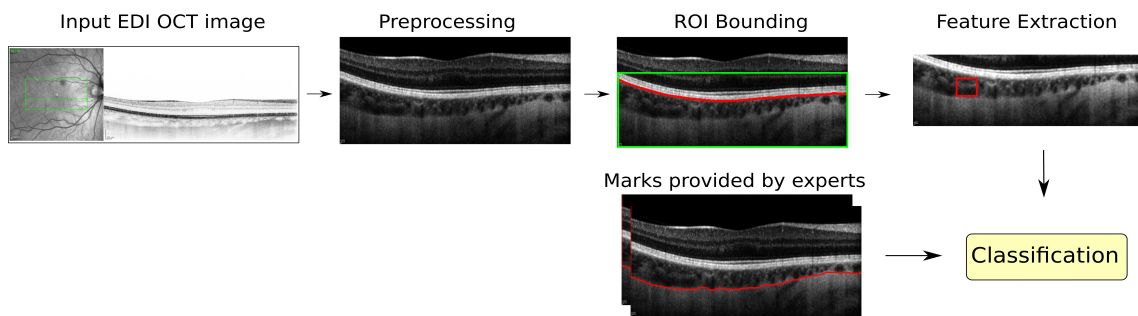
Figure 2: Phases followed for choroid characterization over a sample EDI OCT image.

contour, a new energy term is added, representing the distance between a node and the strongest edge in the area of searching. This term is important to encourage the movement of the contour in the first steps of its evolution.

Regarding the intensity-based information, a term encouraging pixels with bright regions above is defined: accumulated intensity in a range of rows above each pixel in the image is computed; then, those pixels with the highest value per column are extracted and finally, the value of this term is computed as the gradient distance over them. These steps are reflected in Figure 3 (f) (g) and (h), respectively, for an easier understanding.

It is necessary to clarify that, in order to combine different levels of information detail during the process, this model is designed to work over two images at the same time, each one enhanced in a different manner. The first image is the original one smoothed and with enhanced contrast, which contains precise information, while the second image, obtained with an aggressive preprocessing, provides a coarse level of information, useful in the firsts steps of energy minimization.

Using this model, the nodes in the active contour will be attracted to the desired boundary in the image through a process of several stages of minimization. For this boundary, two stages of minimization have been defined, allowing to adjust parameters of the model.

However, given that this method was designed for standard OCT images, it needs to be modified in order to make it feasible for EDI-OCT images. The main difference between images captured with both techniques is that lower layers present higher contrast and definition in case of EDI OCT. Thus, as previous step for RPE-BC/Choroid boundary segmentation, the mentioned model is used to detect the upper boundary of RPE-BC (it corresponds to the strongest edge in the image). Using that information, the active contour used to segment RPE-BC/Choroid

is initialized automatically and the segmentation of the boundary is immediate, considering that it corresponds to a very strong light-to-dark transition. Obviously, parameters of the active contour-based model must be adjusted in order to extend it for this new kind of images.

## 2.3 Choroid Characterization

Once the upper boundary of the choroid is determined, it is necessary to establish its limit with the sclera. Choroid layer presents different features than the rest of layers in the retina. For instance, since choroid is deep underneath the retina, OCT signals can be degraded. This fact, in addition with the weakness presented by choroid lower boundary, makes it almost invisible in most cases. Besides that, its appearance is different from the other layers, because it is formed by a dense vascularity structure and its shape presents greater variations in thickness. In contraposition to that, sclera presents a more homogeneous intensity and it does not present vascularity features.

Considering all these properties, it seems that the detection of this layer can be tackled as a pattern recognition problem, where its texture features can be analyzed to characterize it. With that purpose, after enhancing the image contrast, several windows of $w \times h$ pixels are obtained from the bounded region in the images and are used to extract the different texture descriptors, described in Section 2.3.1 (Figure 4 shows a sample image with some of the extracted windows). Then, the process of classification is performed.

After assessing the performance of the different texture descriptors at the current problem, the method providing best results can be explored more deeply. To do that, a feature selection procedure is applied with the purpose of determining if removing irrelevant or redundant features can involve an improvement in the performance of the classifier.
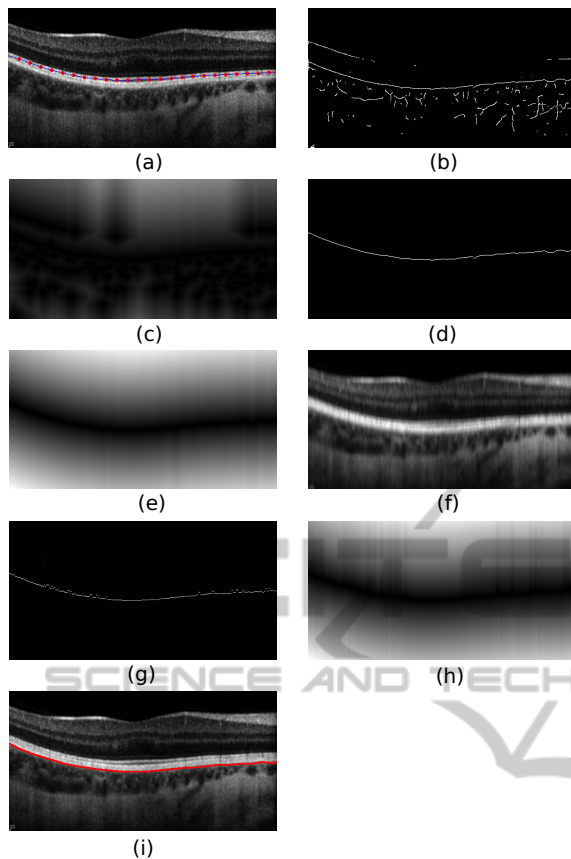
Figure 3: Segmentation of the choroid upper boundary (RPE-BC/Choroid): (a) sample image with initialized active contour; some energy terms: (b) edges corresponding to dark to light transitions; (c) gradient distance computed over (b); (d) strongest edges computed per column; (e) gradient distance computed over (d); (f) accumulated intensities above each pixel; (g) strongest pixels per column in (d); (h) gradient distance computed over (e); (i) boundary given by interpolation of final nodes in the active contour.
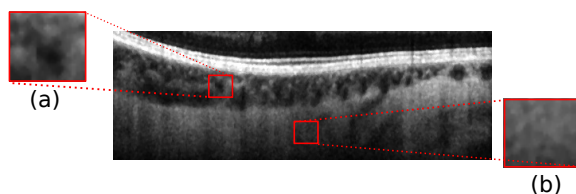


Figure 4: Sample image with extracted windows corresponding to (a) choroid layer and (b) sclera. Zoom has been applied in order to show visual textural differences between both areas (note the different homogeneity presented in both cases).

### 2.3.1 Texture Descriptors

In order to analyze different modalities for texture descriptor extraction, three widely used methods are studied to perform the analysis, each one corresponding to a different modality. Firstly, Markov Random

Fields (MRF) is analyzed, that is a model-based method; then, Co-ocurrences Features is proposed as statistical method and finally, as signal processing method, the Discrete Wavelet Transform (DWT). This last method is chosen also because it is used in previous work (Danesh et al., 2014). Therefore, this study is also useful to determine if the approach chosen in that work is the most appropriate for this task or, on the contrary, there are other methods that can characterize better the choroid layer.

The three considered methods are detailed as follows:

**Markov Random Fields (MRF).** (Besag, 1974) are model based texture analysis methods that construct an image model whose parameters capture the essential perceived qualities of texture. A MRF is a 2D lattice of points where each point is assigned a value that depends on its neighboring values. Thus, MRFs generate a texture model by expressing the gray values of each pixel in an image as a function of the gray values in a neighborhood of the pixel. The neighborhood of a pixel is defined as the set of pixels within a Chebyshev distance $d$. Once the parameters of the model are calculated, the descriptor of an input image is obtained by computing the directional variances proposed in (Çesmeli and Wang, 2001). Notice that for a distance $d$, the descriptor comprises $4d$ features.

**Co-occurrence Features.** (Haralick et al., 1973) are based on the computation of the conditional joint probabilities of all pairwise combinations of gray levels, given an interpixel distance and an orientation. This method generates a set of Gray Level Co-occurrence Matrices, and extract several statistics from their elements. As in the above method, the Chebyshev distance is considered and so, for a distance $d = 1$, 4 orientations are considered ($0^o$, $45^o$, $90^o$ and $135^o$, as diagram in Figure 5 reflects), and 4 matrices are generated. In general, the number of orientations and, accordingly, the number of matrices for a distance $d$ is $4d$. From each co-occurrence matrix a set of 14 statistics are computed, representing features such as homogeneity or contrast. Then, mean and range across matrices are extracted, resulting in a set of 28 features which will be the descriptor of the input image.

**The Discrete Wavelet Transform.** (Mallat, 1989) generates a set of wavelets by scaling and translating a mother wavelet, which is a function defined both in the spatial and frequency domain. The different parameters of the mother wavelet control the bandpass of the filter in order to generate high-pass (H) of
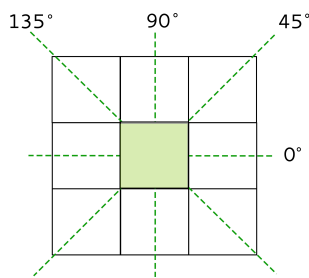
Figure 5: Orientations for distance d = 1 in Co-occurrence Features.

low-pass (L) filters. The wavelet decomposition of an image consists in applying wavelets horizontally and vertically to generate 4 subimages at each scale (LL, LH, HL, HH), which are then subsampled by a factor of 2. After the decomposition, the process is repeated $n-1$ times over the LL subimage, where $n$ is the number of scales of the method. This iterative process results in the so-called standard pyramidal wavelet decomposition shown in Figure 6.

Among the different mother wavelets found in the literature, two of the most popular ones have been used (Daubechies, 1992): Haar is the simplest non-trivial wavelet, and Daubechies is one representative type of basis for wavelets. The descriptor of an input image is obtained by computing the mean and the absolute average deviation of the input and LL images, and the energy of the LH, HL and HH images. Therefore, the descriptor of an input image is composed of $2+5 \times n$ features.
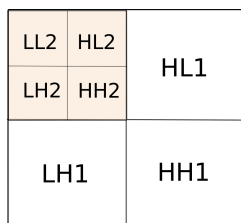


Figure 6: Pyramidal wavelet decomposition for n=2 scales.

### 2.3.2 Classification

After descriptor extraction, they are processed by a classifier, which will determine if a region must belong to choroid layer or not. In this work, a supervised classifier, Support Vector Machine (SVM), has been used. SVM is based on the statistical learning theory, performing classification by constructing an N-dimensional hyperplane that optimally separates the data in categories. Results in terms of percentage accuracy are shown in next section, representing the rate per cent of the windows correctly classified, according to their category (in this case, belonging to choroid layer or not).

### 2.3.3 Feature Selection

Once all textural descriptors have been assessed, a feature selection process is applied over the method providing the best performance. This is motivated by the fact that an appropriate selection of the considered features can lead to an improvement in the classification, not only in terms of speed, but also regarding the generalization capacity or simplicity of the model (Bolón-Canedo et al., 2013). In this work, despite the variety of existing methods for feature selection, filters are chosen, because they are computationally simple and fast. In particular, three filters are considered:

- *INTERACT* (Zhao and Liu, 2009) is a subset filter mainly based on symmetrical uncertainty and the consistency contribution, which indicates how significantly the elimination of a feature can affect consistency.

- *Correlation-based Feature Selection* (Hall, 1999) is a simple multivariate filter that ranks feature subsets according to a heuristic based on correlation. Thus, subsets containing features that are highly correlated with the class and uncorrelated with each other, are selected.

- *Consistency-based Filter* (Dash and Liu, 2003) is based on the evaluation of the worth of a subset of features by the level of consistency in the class values when the samples are projected onto the subset of attributes. The inconsistency criterion allows to determine what extent the dimensionally reduced data can be accepted.

## 3 MATERIAL AND METHODS

The aim of this work is to characterize choroid layer in the OCT retinal images through a texture analysis. The materials and methods used in this research are presented in the text that follows.

### 3.1 Data Source

Experiments have been done over a dataset of 63 two-dimensional EDI OCT retinal images corresponding to 7 different patients. Images were provided by Hospital do Barbanza, Ribeira (Spain) and they were extracted using Spectralis OCT scanner (Heidelberg Engineering). Scanner optic axial resolution is $5\mu m$. Captured images have resolution of $1520 \times 496$ pixels, although after the processes of cropping and resizing applied during the preprocessing phase, their dimensions are reduced to $495 \times 218$ pixels in mean.

## 3.2 Experimental Procedure

The experimental procedure is detailed as follows:

1. Extract windows from the ROI in the images, using marks made by the experts to label them.

2. Apply the three texture analysis methods described in Section 2.3.1 to the dataset of images.

3. Train a SVM (Section 2.3.2) with radial basis kernel and automatic parameter estimation. Since 10-fold cross-validation was used, the average error across all trials was computed.

4. Evaluate the effectiveness of the proposed methodology in terms of accuracy.

5. Apply the feature-selection procedures over the textural method providing the best performance. Repeat steps (3) and (4).

# 4 RESULTS AND DISCUSSION

Two experts have marked the OCB boundary in all images. Windows for descriptor extraction have been obtained and categorized from those areas corresponding to agreement between experts. Window size is $w \times h = 31 \times 31$ pixels, which seems big enough to cover textural information in the choroid layer. Since the number of windows extracted from the sclera area is too much high than those extracted from the choroid in each image, this set is reduced in order to consider balanced sets. Regarding the texture descriptors used in this work, distances covering range 1 to 7 are studied for Markov Random Fields and Co-occurrence Features, whereas for DWT, 4 scales and 4 different wavelets are used. Results are shown in Tables 1, 2 and 3. Best rate for each method has been highlighted.

Table 1: Accuracy(%) using SVM classifiers for Markov Random Fields with distances $d$ from 1 to 7.

| 1 | 2 | 3 | 4 | 5 | 6 | 7 |
|---|---|---|---|---|---|---|
| **80.52** | 79.59 | 71.99 | 77.48 | 77.38 | 74.67 | 75.35 |

Table 1 presents results for Markov Random Fields, whose best rate is obtained for distance $d = 1$ (over 80%). Besides that, it is possible to observe that bigger the distance, the lower the accuracy, what means that textural information is progressively smaller in those cases.

Co-occurrence Features (Table 2) provides rates over 90% in all cases. In particular, the highest accuracy is near 94% and it is obtained using distance $d = 3$.

Table 2: Accuracy(%) using SVM classifier for Co-ocurrences Features for distances $d$ from 1 to 7

| 1 | 2 | 3 | 4 | 5 | 6 | 7 |
|---|---|---|---|---|---|---|
| 93.88 | 93.80 | **93.97** | 93.76 | 93.62 | 93.26 | 93.32 |

Table 3: Accuracy(%) using SVM classifier for Discrete Wavelet Transform, considering different mother wavelets with scales $n$ from 1 to 4. Daub$i$ represents the Daubechies orthonormal wavelet, with number of vanishing moments equal to half the coefficient $i$. Note that the Haar wavelet is equivalent to Daub2.

|  | 1 | 2 | 3 | 4 |
|---|---|---|---|---|
| Haar | 86.86 | **88.68** | 82.95 | 80.05 |
| Daub4 | 86.11 | 84.02 | 82.58 | 79.42 |
| Daub6 | 85.68 | 84.31 | 81.73 | 78.39 |
| Daub8 | 85.66 | 85.86 | 82.08 | 78.82 |

Regarding DWT, Table 3 shows that using Haar wavelet with $n = 2$ scales provides the best result (88.68%). Results also reflect that performance decreases at the time that distance increases. This is due to the window size chosen for this work, given that when more scales are used, information in the smallest LL subimages is degraded. Therefore, studying more scales does not make any sense.

Though all considered texture analysis methods present acceptable rates, the highest accuracy (93.97%) is obtained using Co-occurrence Features with distance $d = 3$. Besides that, this method provides, in general, better and more stable results. Regarding Markov Random Fields, most results are worse than those provided by the other considered methods. Despite the fact that both Markov Random Fields and Co-occurrence Features uses information of the pixel's neighborhood, it is possible to conclude that MRF does not work so well because the statistics proposed by Haralick et al. provide much more information. With regards to DWT, which was specially interesting because Haar wavelet was used in the mentioned previous work (Danesh et al., 2014), it presents lower accuracy (always below 90%) than Co-ocurrences in all cases.

Table 4: Results using SVM classifier for Co-occurrence Features with distance $d = 3$, after applying filters for feature selection: first row shows number of selected features whereas the accuracy is shown in second row.

|  | No FS | INT | CFS | Cons |
|---|---|---|---|---|
| N. Features | 28 | 14 | 9 | 15 |
| Accuracy (%) | 93.97 | 93.18 | 91.35 | 93.84 |

Since the method providing the best results, Co-occurrence Features, considers features that may be strongly correlated (Haralick et al., 1973), the feature-selection process proposed in Section 2.3.3 is motivated. Thus, filters described in that section are consi-

dered in order to remove irrelevant features. They are applied to the features extracted using Co-occurrence Features with distance $d = 3$, since this method, as it was commented, provides the best performance. After feature selection, process described in Section 2.3.2 is repeated: SVM is trained and a 10-fold cross-validation is done. Table 4 shows accuracy obtained by each method (INTERACT - INT, correlation-based feature selection - CFS and consistency-based filter - Cons), as well as the number of features selected by each one.

As it was commented previously, Co-occurrence Features with distance $d = 3$ provides the best rate (93.97%). For this descriptor, 28 features are considered. Results after applying feature selection, presented in Table 4, show that CFS has the most aggressive behaviour since it retains 32.14% of the features, but at the expense of a slight decrease in the accuracy of the classifier, while Cons and INTERACT retain around the 50% of the initial features with no degradation in performance. Thus, results obtained with Co-occurrence Features ($d = 3$) can be remained but with a significant reduction in the number of features. Note that a reduction in the number of feature implies a decrease in the time needed to compute the descriptor. This time, which is not a matter of study in this paper, could become a bottle neck when applying a segmentation process in which a great amount of windows have to be analyzed, and herein also lies the relevance of using feature selection.

## 5 CONCLUSIONS AND FUTURE WORK

In this work, an automatic characterization of the choroid layer in EDI OCT retinal images based on textural information has been presented. The method consists in locating the region of interest through an active contour-based segmentation and then, extracting texture descriptors to perform a classification process with the purpose of discriminating between regions belonging to the choroid from those corresponding to other areas. Different texture descriptors have been considered for the pattern recognition task in order to perform a comparative study and determine the best one to represent this layer. Results show that the choroid can be identified in a very effective way using Co-ocurrences Features, surpassing previous works (Danesh et al., 2014). Feature selection has been applied, allowing to eliminate the irrelevant/redundant features with no degradation in the accuracy of the performance. Therefore, texture information extracted with this method can be used to

characterize this layer in a robust way.

As future work, a deeper study of textural information with different descriptors could be done, as well as more classifiers can be considered. Besides that, this information must be included in a methodology that allows to tackle the accurate segmentation of the lower choroid boundary.

## ACKNOWLEDGEMENTS

## REFERENCES

Alonso-Caneiro, D., Read, S. A., and Collins, M. J. (2013). Automatic segmentation of choroidal thickness in optical coherence tomography. *Biomed. Opt. Express*, 4(12):2795–2812.

Besag, J. (1974). Spatial interaction and the statistical analysis of lattice systems. *Journal of the Royal Statistical Society. Series B*, 36:192–236.

Bill, A., Sperber, G., and Ujiie, K. (1983). Physiology of the choroidal vascular bed. *Int. Ophthalmol.*, 6(2):101–107.

Bolón-Canedo, V., Snchez-Maroo, N., and Alonso-Betanzos, A. (2013). A review of feature selection methods on synthetic data. *Knowl. Inf. Syst.*, 34(3):483–519.

Çesmeli, E. and Wang, D. L. (2001). Texture segmentation using gaussian-markov random fields and neural oscillator networks. *IEEE Transactions on Neural Networks*, 12(2):394–404.

Danesh, H., Kafieh, R., Rabbani, H., and Hajizadeh, F. (2014). Segmentation of choroidal boundary in enhanced depth imaging octs using a multiresolution texture based modeling in graph cuts. *Computational and Mathematical Methods in Medicine*, 2014(479268).

Dash, M. and Liu, H. (2003). Consistency-based search in feature selection. *Artificial Intelligence*, 151(1-2):155–176.

Daubechies, I. (1992). *Ten Lectures on Wavelets*. Society for Industrial and Applied Mathematics, Philadelphia, PA, USA.

Dhoot, D., Huo, S., Yuan, A., Xu, D., Srivistava, S., Ehlers, J., Traboulsi, E., and PK., K. (2013). Evaluation of choroidal thickness in retinitis pigmentosa using enhanced depth imaging optical coherence tomography. *British Journal of Ophthalmology*, 97(1):66–9.

González, A., Ortega, M., Penedo, M., and Charlón, P. (2014). Automatic robust segmentation of retinal layers in oct images with refinement stages. In *International Conference on Image Analysis and Recognition (ICIAR)*, volume 8815 of *Lecture Notes in Computer Science*, pages 337–349. Springer Berlin Heidelberg.

Hall, M. (1999). *Correlation-based Feature Subset Selection for Machine Learning, PhD dissertation*. PhD thesis, University of Waikato.

Haralick, R., Shanmugam, K., and Dinstein, I. (1973). Textural features for image classification. *IEEE Transactions on Systems, Man, and Cybernetics*, 3(6):610–621.

Hu, Z., Wu, X., Ouyang, Y., Ouyang, Y., and Sadda, S. (2013). Semiautomated segmentation of the choroid in spectral-domain optical coherence tomography volume scans. *Investigative Ophthalmology & Visual Science*, 54(3):1722–9.

Imamura, Y., Fujiwara, T., Margolis, R., and Spaide, R. (2009). Enhanced depth imaging optical coherence tomography of the choroid in central serous chorioretinopathy. *Retina*, 29(10):1469–73.

Kajić, V., Esmaeelpour, M., Glittenberg, C., Kraus, M. F., Honegger, J., Othara, R., Binder, S., Fujimoto, J. G., and Drexler, W. (2013). Automated three-dimensional choroidal vessel segmentation of 3d 1060 nm oct retinal data. *Biomed. Opt. Express*, 4(1):134–150.

Lu, H., Boonarpha, N., Kwong, M., and Zheng, Y. (2013). Automated segmentation of the choroid in retinal optical coherence tomography images. In *IEEE Eng Med Biol Soc*, pages 5869–72.

Mallat, S. G. (1989). A theory for multiresolution signal decomposition: The wavelet representation. *IEEE Trans. Pattern Anal. Mach. Intell.*, 11(7):674–693.

Puzyeyeva, O., Lam, W. C., and Flanagan, J. e. a. (2011). High-resolution optical coherence tomography retinal imaging: A case series illustrating potential and limitations. *J. Ophthalmology*, pages 764183–6.

Yin, Z. Q., Vaegan, T. J., Millar, T. J., Beaumont, P., and Sarks, S. (1997). Widespread choroidal insufficiency in primary open-angle glaucoma. *Journal of Glaucoma*, 6(1):23–32.

Zhang, L., Lee, K., Niemeijer, M., Mullins, R., Sonka, M., and Abrmoff, M. (2012). Automated segmentation of the choroid from clinical sd-oct. *Investigative Ophthalmology & Visual Science*, 53(12):7510–9.

Zhao, Z. and Liu, H. (2009). Searching for interacting features in subset selection. *Intell. Data Anal.*, 13(2):207–228.